2.11 Status of the CLIC Damping Rings Design

Yannis Papaphilippou, CERN, CH 1211 Geneva 23, Switzerland
for the CLIC damping rings design team
Mail to: yannis@cern.ch

2.11.1 Generation of Ultra-low Emittances

The high luminosity of a linear collider, at the lowest power, requires the generation of ultra-low emittance high-intensity bunches, with remarkable stability. Although conventional electron sources and positron production schemes provide the intensity required but with emittances that are several orders of magnitude larger than the ones needed. The natural synchrotron radiation damping of the beam when circulating in rings is the cooling mechanism enabling to reach these small emittances.

Table 1: CLIC versus ILC and NLC parameters driving the DRs design.

Parameter [unit]	*ILC*	*NLC*	*CLIC*
Bunch population [10^9]	20	7.5	4.1
Bunch spacing [ns]	369	1.4	0.5
Number of bunches/train	2625	192	312
Number of trains	1	3	1
Repetition rate [Hz]	5	120	50
Horizontal normalized emittance [nm.rad]	4400	2400	500
Vertical normalized emittance [nm.rad]	20	30	5
Longitudinal normalized emittance [keV.m]	38	11	6

The performance challenges of these damping rings (DRs) are driven by the key performance parameters of the collider and the requirements of the upstream and downstream systems, and principally the efficiency of the main linac RF. The parameters guiding the design of ILC [1], NLC [2] and CLIC damping rings are presented in Table 1. The technological choice of super-conducting over copper RF cavities for the main linacs, clearly diversifies the design of damping rings, although a number of design issues and challenges still remain common. In the one flavour of the damping rings as CLIC or NLC, the bunch trains are relatively short with even shorter bunch spacing and with a high repetition rate. The ILC bunch train is much longer necessitating a much longer ring circumference where the train is compressed and uncompressed in a bunch-by-bunch beam transfer scheme. For getting the high luminosity in the ILC, the bunch charge is much higher whereas CLIC targets for much smaller emittances, orders of magnitude lower in all three dimensions (500nm.rad horizontal, 5nm.rad vertical and 6keV.m longitudinal). Although these emittances are unprecedented, modern X-ray storage rings in operation or construction phase are rapidly approaching these regimes. Especially for the vertical emittance, requiring challenging magnet alignment tolerances and stringent control of the optics and orbit, X-ray rings hold the current record, at the level of below 1pm.rad [3-4], thereby reaching the CLIC DR target. Figure 1 presents the horizontal and vertical normalized emittance in a number of low emittance rings, including test facilities, DRs, B-factories and synchrotron light sources, under operation (red) or in the design phase (blue). Whereas

the future light source projects are aggressively pushing the limits of horizontal emittance below 100pm, and some operating ones reach a very low vertical one, CLIC DRs are unique for being in the cross section of both challenges.

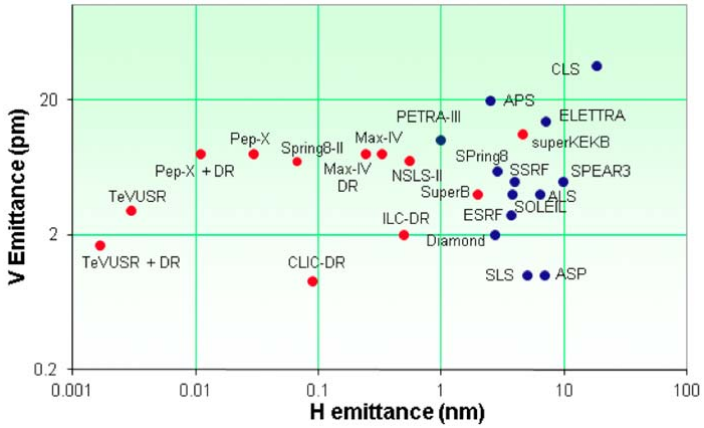

Figure 1: Horizontal versus vertical normalized emittance for low emittance rings in operation (blue) and in the design phase (red) (from R. Nadolski [3]).

2.11.2 **The CLIC Damping Rings Complex**

A schematic layout of the CLIC damping ring complex is shown in Fig. 2 comprising of two pre-damping rings, two damping rings and a delay loop. Two pre-damping rings (PDRs) are needed due to the large input emittance especially coming from the positron source and the high repetition rate of 50Hz. The electron pre-damping ring could become obsolete provided that the delivered electron normalised emittance from the linac can be below 50μm (the horizontal emittance achieved in the PDR).

At every machine cycle, two trains are injected in the damping rings with twice the nominal bunch separation (1 vs 0.5ns), in order to reduce the transient beam loading effects in the RF cavities. The head of each train is separated by half of the damping rings circumference. The two trains are damped simultaneously and then extracted in a single turn from the main damping rings. A delay and recombination loop, downstream of the main rings, is used in order to provide a unique train with the required 2GHz bunch structure.

Standard transport lines transfer the beam between the injector linac, the damping rings, the delay loop and the booster linac. As the train recombination is provided by the same loop for both species, the time delay between the e^+ and e^- trains is recovered in the downstream systems.

2.11.3 **Damping Ring Challenges and Parameter Choice**

The goals guiding the design of the damping rings are driven by the main parameters of the collider and the requirements of the upstream and downstream systems.

The large energy spread of the positron beam reduces the capture efficiency in the pre-damping rings and explains the much larger bunch population needed at their entrance. Note also that the transverse emittances for the two particle species differ by almost three orders of magnitude. For electrons before and after the pre-damping rings, the bunch population contains roughly a 10% overhead for ring and transfer losses.

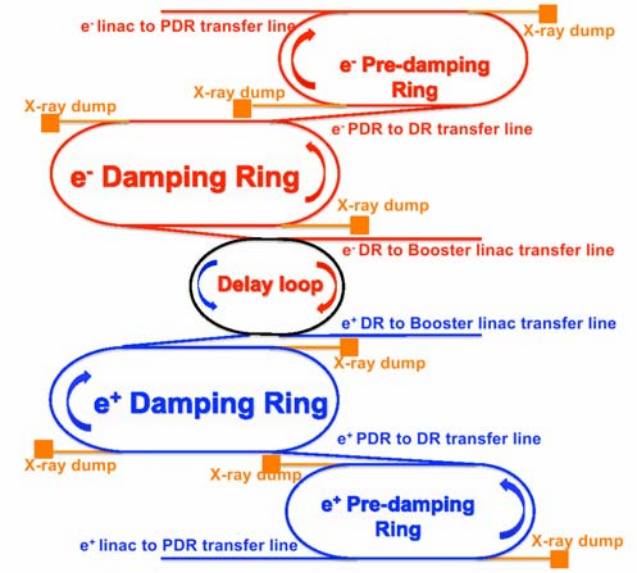

Figure 2: The damping ring complex layout including two pre-damping rings, two damping rings and a single delay loop.

For the pre-damping rings, the main challenge is the huge positrons emittance to be captured, necessitating large dynamic transverse and momentum acceptance [6].

The design challenges of the CLIC main DRs are driven from the extremely high bunch density, i.e. the ratio between bunch charge and the 3-dimensional beam volume, and the collective effects associated with it. In this respect, the CLIC DR parameters shown in Table 2 are carefully chosen and optimised in order to mitigate these effects. In addition, these parameters drive the technology of a number of components such as wigglers, RF system, kickers, vacuum, instrumentation and feedback.

After the adaptation of the latest main linac RF systems parameters, which drive the design of most CLIC accelerator systems, the damping rings presented a final emittance with a blow-up of a factor of 5 in the horizontal emittance due to the effect of IBS [7]. The design strategy followed was to raise the ring energy, change the optics, adapt the wiggler parameters and increase slightly the longitudinal emittance in order to mitigate as much as possible the IBS effect, down to a factor of 1.5, with respect to the equilibrium horizontal emittance. In particular, the scaling of the ratio between the steady state and zero current emittances with the energy is shown in the left part of Fig. 3. The IBS effect is reduced for higher energies as expected. The dependence of the steady state emittances to the energy is displayed on the right part of Fig.3. A broad minimum is observed around 2.0 GeV for the horizontal and vertical emittances, where the IBS effect also becomes weaker. Although higher energies may be also interesting for reducing further collective effects, the output emittance is strongly increased due to the domination of quantum excitation. In this respect, the energy of 2.86 GeV was chosen for the CLIC DR, which is close to a steady state emittance minimum but also reduces the IBS impact [7,8].

Table 2: CLIC Damping Rings' design parameters.

DR Parameters [unit]	*Value*
Energy [GeV]	2.86
Circumference [m]	427.5
Energy loss/turn [MeV]	4.0
RF voltage [MV]	5.1
Compaction factor	1.3×10^{-4}
Damping time transverse / longitudinal [ms]	2.0/1.0
Number of arc cells/wigglers	100/52
Dipole/wiggler field [T]	1.0/2.5

The lattice including the number of cells, the bending magnet characteristics, the wiggler field and period are chosen such that the target emittance is reached within the high repetition rate of 50Hz, in a compact ring. In particular, the wigglers have to reach peak fields that only super-conducting materials can provide them. The vertical emittance at "zero current" is dominated more by vertical dispersion and less by coupling, so in order to achieve it, apart from tight alignment tolerances, a very good correction and control of the orbit is necessary. In any case, the geometrical target emittance of less than 1pm.rad is the present achieved record in synchrotron light source storage rings for similar energies and bunch currents [4].

Due to the very small beam size especially in the vertical plane, the space charge tune-shift can be quite important. For reducing it, and apart from the short ring circumference, the bunch length had to be increased to the maximum acceptable level imposed by the RTML, by tuning the TME cell to an increased momentum compaction factor.

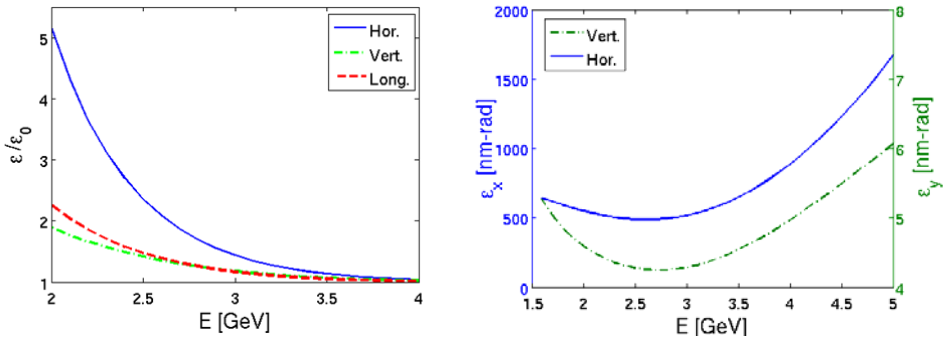

Figure 3: Dependence of the IBS growth factor, i.e. ratio between steady state and equilibrium emittances (left) and steady state emittances (right) with energy.

The beam loading transients in the RF cavities can be reduced by halving the RF frequency, which indeed imposes injection of two trains with a subsequent recombination in a delay loop. In order to reduce the stationary phase and linearise the bucket, the voltage cannot be raised without shortening the bunch. Instead, the energy loss per turn was increased in a way that it does not affect the fast damping, by reducing the bending field.

High bunch density in combination with the short bunch spacing triggers two stream instabilities. In the electron ring, the fast ion instability can be avoided with ultra-low

vacuum pressure. This necessitates coating of vacuum chambers with getters like NEG for increasing pumping in addition to vacuum conditioning.

In order for the electron cloud build up to be reduced and the instability not to occur in the positron ring, it is necessary that the vacuum chambers present a low secondary electron and photo-emission yield (SEY and PEY). The low SEY can be achieved with special chamber coatings, whereas the low PEY is already imposed by the required absorption efficiency to reduce the heat deposition in the super-conducting magnets. In addition, the increased bunch spacing with the two trains scheme, indeed relaxes the above requirements.

The stringent beam stability requirement of typically 10% of the beam size, imposes tight jitter tolerances for the damping ring extraction kicker (a few 10^{-4}). An ILC type beam extraction experiment using a proto-type strip-line kicker has been carried out at KEK-ATF [13] with quite encouraging results, approaching the stability requirements of CLIC.

2.11.4 **Optics Design**

The optics functions for a quarter of the ring, are shown in Fig. 4. Each arc is filled with 48 TME cells and 2 half cells at either side for the dispersion suppression. The original TME cell was designed as compact as possible but presented several weaknesses with respect to space and magnet strength constraints. A series of optimisation steps was followed in order to rationalise it and, at the same time, to reduce the effect of IBS [9]. The major contribution of IBS is associated to locations where the beam sizes, i.e. beta functions and dispersions, reach their minima. In the TME cell, both horizontal and vertical beam sizes become minimum at the centre of the arc cells and it is exactly at this location where IBS growth rates are maximum. However, the low emittance condition requires only small horizontal betatron function in the bending magnets while the vertical one can be large.

A defocusing gradient in the bending magnet can reduce further the emittance but also reverses the behaviour of the vertical beta at the centre of the dipole (Fig.4) , hence reducing the IBS growth rate, while the resulting output emittance is almost the same [9].

As the final emittance of the ring can be further reduced by the use of damping wigglers in the straight sections, which provide also the fast damping, a detuned TME cell was designed, which is more flexible, easier to achieve and has lower chromaticity. The horizontal and vertical phase advances are $\mu_x = 0.408$ and $\mu_y = 0.005$. The horizontal phase advance allows a higher value of the momentum compaction factor, while keeping the final emittance within the budget. The vertical one is the smallest possible in order to increase the vertical beta functions and reduce IBS kicks while keeping the beam acceptance large enough. The bending radius of the dipole (determining its field of 1 T and length of 0.58 m) was chosen such that the energy loss per turn becomes smaller and the bunch length as large as possible.

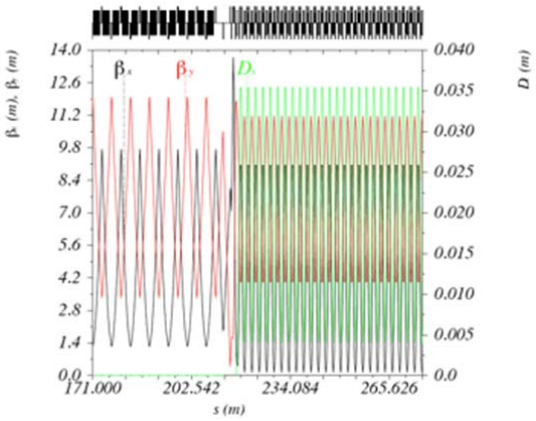

Figure 4: Horizontal (black) vertical (red) beta functions and horizontal dispersion (green) of the for a quarter of the CLIC DR.

The long straight sections (LSS) are filled with FODO cells and accommodate the damping wigglers. There are 13 FODO cells per straight section with two wigglers per cell. Further emittance minimisation can be made by properly choosing the lattice functions in the wigglers [9]. For a FODO cell, the minimum emittance is reached for horizontal phase advance $\mu_x = 0.31$ and for the vertical one tending to zero. The vertical phase advance can then be set as low as possible ($\mu_y = 0.12$) in order for the chromaticity to be minimized. Another possible choice is $\mu_y = 0.25$ corresponding to minimum vertical betas and thus, maximum vertical acceptance.

The lattice functions between the arcs and the straight sections are matched with the dispersion suppressors and matching sections. The first part is a half TME cell, with different quadrupole strengths. These two quads are used as knobs in order to minimise the length of the suppressor. A dipole is then used for the suppression of the dispersion and four more quads as knobs for matching all the optics functions at the entrance of the LSS. Space is reserved in the dispersion free region for injection/extraction and RF cavities. This lattice including sextupoles, magnet fringe fields and linear imperfections was proved to provide an adequate dynamic aperture [11] and good low emittance tuning characteristics [12].

2.11.5 **Wiggler Specifications and Performance**

Producing the ultra-low horizontal emittance in a compact ring within the machine pulse of 20 ms necessitates the use of damping wigglers. The highest field and relatively short period is needed in order to reach the target emittances. Pure permanent magnets are not able to reach high field (the maximum is around 1.2 T for Sm_2Co_{17}), so pole concentrators are used (e.g. vanadium permendur) to enhance the field to a maximum value of 2.3 T. This maximum field of 2.3T can be reached for a relatively large period of around 140 mm. In that case, the horizontal emittance gets more than doubled and far above the required 500 nm. In order to achieve the target DR performance, the number of wigglers has to be more than doubled, which results to a 40% increase of ring circumference. In this respect, the only way to reach the very small emittance while keeping the ring compact, is the use of high field for high gap/period ratio, necessitating superconducting damping wigglers.

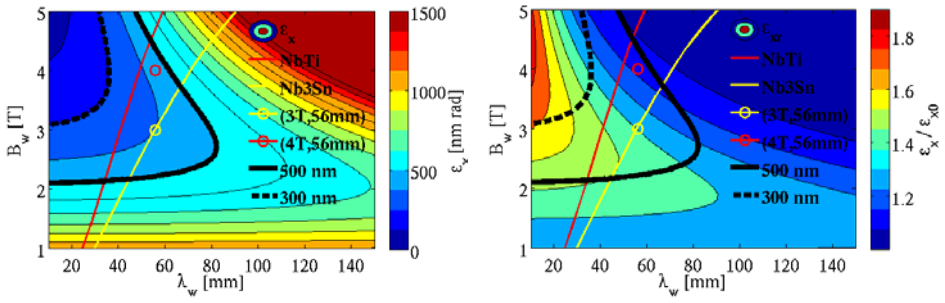

Figure 5: Dependence of the steady state emittance (left) and its ratio with the equilibrium emittance (right) as a function of the wiggler peak field and period. The blue color denote smaller emittances or ratios, whereas the red ones bigger. The black curve traces the horizontal emittance target barrier of 500nm.

In order to explore the dependence of wiggler characteristics on the output horizontal emittance with respect to IBS, a simulation was performed by varying the wiggler peak field and period, while keeping the final vertical and longitudinal ones fixed. The results are shown in Fig. 5. The left plot is colour-coded with the horizontal steady state emittance while the right one with the ratio between the steady-state and the zero-current one. The black curve corresponds to the target emittance of 500 nm and defines the area for which the output emittance is within the budget. The highest field and the shortest period is necessary for reaching the smallest emittance possible. On the other hand, the effect of IBS in that case becomes extremely strong. For reducing the blow-up due to IBS, still the highest fields are interesting but for moderate periods.

In each DR, it is foreseen to install 52 wigglers of peak field 2.5 T and 50 mm period, based on NbTi technology. A short prototype with these characteristics was developed and measured at Budker Institute achieving the field requirements. Another mock-up with more challenging design (2.8 T field, with 40 mm period) wound with Nb_3Sn wire is also under testing at CERN [13].

Around 9kW of total power is produced by each wiggler and an absorption system is necessary and critical to protect machine components and wigglers against quench, but also to lower the photo emission yield for reducing the e-cloud effect in the positron ring. The power limit is set between 1 and 10 W/m, depending the wire technology and the vacuum chamber cooling. A series of horizontal and vertical absorbers are placed downstream of the wigglers. A terminal absorber at the end of the long straight section is absorbing the remaining 100kW of photon power [14].

Full wiggler prototypes with similar magnetic characteristics are expected to be built at BINP and installed at a straight section of the ANKA synchrotron for tests under beam conditions, during 2014. Of particular interest would be the validation of cooling concept and the resistance of the wiggler to heat load under real beam conditions.

2.11.6 **Longitudinal and RF Parameters**

The very high peak and average current corresponding to the full train of 312 bunches spaced by 0.5 ns presents a big challenge due to the transient beam loading, especially for a 2 GHz RF system. In this respect, it was decided to consider two bunch trains with 1ns bunch spacing. The RF system with frequency of 1 GHz is more

conventional and an extrapolation from existing designs is possible. Nevertheless, the trains have to be recombined in a delay loop downstream the DRs with an RF deflector.

This choice has a positive impact in both the PDRs and the main DRs. Doubling the bunch spacing halves the harmonic number increasing the momentum acceptance. The extraction kicker rise time becomes shorter but it is still long enough (560 ns). The 2-train structure may require two separate extraction kicker systems or one kicker with longer flat top (1 μs). The beam loading is significantly reduced, as the larger bunch spacing reduces peak current and power by a factor of 2. Several beam dynamics issues are also eased due to double bunch spacing. The e-cloud production and instability is reduced, while the fast ion instability will be less pronounced by doubling the critical mass above which particles get trapped. The reduced number of bunches per train reduces the central ion density, the induced tune-shift and the rise time of the instability is getting doubled, thus relaxing the feedback system requirements. Finally, a bunch-by-bunch feedback system is more conventional at 1 than at 2 GHz.

For both frequencies, and in order for the RF bucket to become more linear, the stationary phase has to be kept low. This could be achieved be increasing the RF voltage but this shortens the bunch and increases the impact of collective effects. In order to lower the stationary phase, the dipole field was lowered for reducing the energy loss per turn. At the same time, the momentum compaction is increased and so does the bunch length, leaving some margin for the increase of the voltage.

2.11.7 **Collective Effects**

2.11.7.1 ***Intrabeam Scattering***

One of the main limitations of the CLIC DRs is the effect of intrabeam scattering (IBS) which increases the output emittances in all three dimensions. IBS is a small angle multiple Coulomb scattering effect which depends on the lattice characteristics and the beam dimensions. It is described by a series of theories and approximations [15-18]. Multi-particle tracking codes were developped [19,20] was developed for evaluating the IBS effect in the emittance, including damping and quantum excitation. These codes were compared with classical IBS theories and approximations and the results are presented in Fig.6. for the horizontal emittance evolution over one turn of the ring. The results seem to be in very good agreement with the Piwinski theory, while all other theories are very close to the simulations. In addition, the trend of the emittance evolution is the same. Due to this identical behaviour of the theories and simulations in the arcs and straight sections of the DR, and taking into account that the simulations are quite lengthy, it is convenient to use one of the analytical approaches for understanding and minimising the IBS effect. Thus, the Piwinski theory is used for this purpose, as it seems to be the closest to the simulation results [8].

A measurement campaign in CESRTA [21] and SLS [22] has been initiated for evaluating IBS effect and benchmark theories and simulation codes.

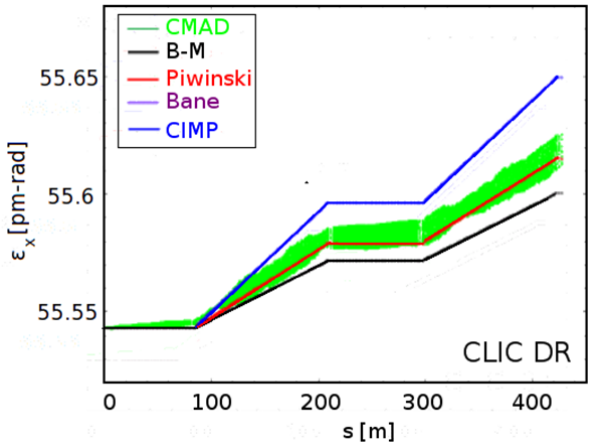

Figure 6: The one turn behaviour of the horizontal emittance starting from the zero current values, as computed by CMAD-IBSTrack (green), BM (black), modified Piwinski (red), Bane (purple) and CIMP (blue) formalisms.

2.11.7.2 *Space Charge*

Due to the very small beam size especially in the vertical plane, the space charge tune-shift can be quite large, and an effort was undertaken in order to reduce the vertical tune-shift to around 0.1. In this respect, the bunch charge and the beam sizes cannot be changed without affecting the collider's performance and the energy was already optimised for reducing the relative impact of IBS, while reaching the required steady state emittances. Consequently, in order for the space charge to be reduced, the ring has to become as compact as possible. At the same time, the bunch length has to be increased without affecting the performance of the downstream bunch compressors. This was achieved by increasing the equilibrium bunch length through combined reduction of the circumference (removing wiggler cells), lowering the harmonic number by reducing the RF frequency and increasing the momentum compaction factor. Note finally that the space charge tune-shift grows to its final large value during the first few ms of damping to the steady state emittance thus forcing the beam core to traverse resonances. Fast pulsing quadrupoles may be necessary, in order to control the coherent tune-shift in order to avoid emittance growth or beam loss.

2.11.7.3 *Electron Cloud Effect and Mitigation*

The positron DR accumulates many densely populated bunches with a narrow spacing. Therefore, electron cloud could be an issue as the positron beam emits synchrotron radiation photons, which create a large number of photoelectrons at the inner chamber wall surface which get scattered inside the vacuum chamber and they can multiply through secondary emission. This causes electrons to be accumulated in the chamber in large amounts with a possible destabilising effect on the circulating beam.

The electron cloud build up was simulated with Factor2 code [23], for elliptical beam pipes. In the dipoles, the electron cloud formation appeared to be largely dominated by the photoemission up to maximum secondary emission yields of 1.8 with central densities between 10^{11} to 10^{13} m^{-3}.

In the wigglers, the situation is more critical because of the smaller pipe radius. The electron cloud build up starts to be dominated by secondary emission for maximum

SEY's around 1.5. Fig. 7 show the electron central densities for three different values of photoemission yield of 90, 99% or 99.9% and maximum SEY of 1.3, 1.5 and 1.8. These studies show that, independently of the initial seed of photoelectrons, extremely high central densities of electrons can be reached for SEY of 1.8. For SEY of 1.3, the electron central density would still be very high if the absorber absorbs less than 99.9% of the emitted synchrotron radiation. Therefore, for maximum SEY below 1.3, the photoelectrons can still be present in large numbers in the wiggler beam pipe, if the absorption is not sufficiently efficient to remove a high fraction of them.

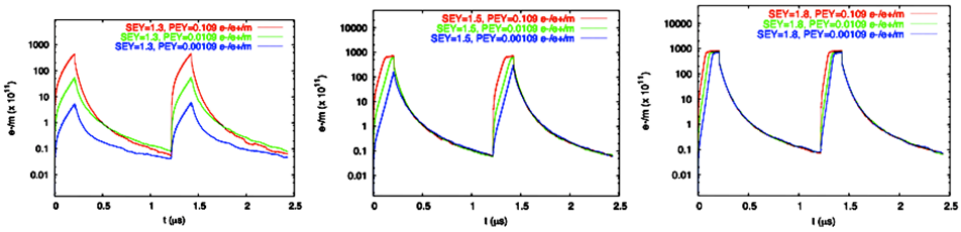

Figure 7: Electron central densities in the wiggler chamber of the CLIC DRs for photoemission yields of 90 (red), 99 (green) or 99.9\% (blue) and secondary electron yield of 1.3 (left), 1.5 (center) and 1.8 (right).

The single bunch electron cloud instability has been studied with an intense simulation campaign showing that the threshold value for the e-cloud density lies at about $5x10^{13}m^{-3}$ in the wigglers, independently of the electron density value in the dipoles. This means that countermeasures are needed to prevent electron accumulation in the wigglers, because when the electron cloud forms it reaches very quickly the critical values to make the beam unstable.

Conventional feedback systems cannot damp the e-cloud instability, as a very wide band is needed. Several mitigation techniques are presently under study[3], including low impedance clearing electrodes, solenoids (only usable in field free regions), low SEY surfaces, grooved surfaces and coatings with NEG and TiN. In particular, an amorphous carbon coating has been extensively tested at SPS [24] and later at CESRTA [25], with promising results, with respect to SEY and photo emission.

It has to be noted that some techniques such as surface coatings, non smooth surfaces or clearing electrodes to fight electron cloud do not come for free and can be serious high frequency impedance sources [26].

2.11.7.4 *Ion Effects*

In the electron DR, the ion oscillation frequency inside the bunch train during the store is in the range of 300 MHz (horizontal plane) to about 1 GHz (vertical plane), to be divided by the the square root of the mass number of the ion However, not all ion types will be trapped in the bunch train and the ones trapped around the beam are those having a mass number above a critcal value, which depends on the location in the ring (due to the different beam sizes). Molecules like N_2 and CO can be trapped almost along the full ring and will accumulate around the electron beam, potentially becoming a source of fast ion instability. The critical masses for trapping are twice as large, reducing the fraction of the ring over which ions like H_2O can be trapped. With the pressure of 1nTorr, the induced tune shift introduced by the ion cloud at the end of the train is moderate. The exponential rise time of the fast ion instability is quite large and equal to a few turns for both options. It would therefore require a very demanding

multi-bunch feedback system to be controlled and/or an even lower vacuum pressure through coatings with getters (NEG) or conditioning. The train gaps have also proved to provide a natural cleaning mechanism for the trapped ions.

2.11.7.5 *Instabilities and Impedance Budget*

The broad-band model is used as a first approximation to model the whole ring in order to scan over different impedance values and define the instability threshold and the impedance budget. In these model, the impedance source is assumed to be identical in the horizontal and vertical planes.

In the transverse plane, a strong head-tail instability or Transverse Mode Coupling Instability (TMCI) can occur and cause rapid beam loss. In the case of a round beam and axisymmetric geometry for a short bunch an analytical criterion can be used to predict the TMCI threshold of around 10.7 MΩ/m for the transverse broad-band resonator in the vertical plane.

Simulating the evolution of the bunch centroid for zero chromaticity over several turns for different impedance values, it was found that modes 0 and -1 are observed to move and couple for impedance values of 15 MΩ/m and 4 MΩ/m in the horizontal and vertical plane respectively, causing a TMCI.

Chromaticity is believed to raise the TMCI threshold thanks to the tune spread that it causes and because it locks the coherent modes to their low intensity values, making mode merging weaker. For this reason, a simulation was done for different positive and negative values of chromaticity. As expected, the presence of chromaticity causes the modes to move less and not to merge and by consequence to avoid a TMCI, but another type of instability, the head-tail instability, is occurring. The TMCI quickly becomes very fast above the threshold for the onset, but for the case of head-tail instability the calculation of its rise time is needed and the damping time of 2 ms defines an instability threshold at 2MΩ/m.

The resistive wall in the wiggler sections with 6 mm vertical half aperture is expected to be a strong source of impedance. Because of the small aperture, compared to 9 mm for other parts of the ring, the contribution of the wigglers is expected to take a significant fraction of the available impedance budget. Moreover, layers of coating materials, which are necessary for e-cloud mitigation or good vacuum, can significantly increase the resistive wall impedance especially in the high frequency regime. The materials used in these simulations are stainless steel (ss) and copper for the pipe of the wigglers, which is assumed to be flat. Amorphous carbon (aC), used for e-cloud mitigation, and non-evaporated getter (NEG), used for good vacuum, were chosen as coating materials. Different material and coating combinations were tried, in order to study the effect of coating on the threshold. For the case of copper, the thresholds are higher compared to those of stainless steel making it a better choice in terms of instabilities but also a more expensive material. Adding a layer of coating material on the beam pipe reduces the intensity thresholds and in fact the thicker the coating is, the more the threshold is reduced, corresponding to an extra 1MΩ/m reduction in the impedance budget.This budget is expected to be further reduced if all the different contributions from the DR are taken into account.

The rise time of the coupled bunch modes caused by resistive wall are estimated to be 0.3 ms corresponding to about 210 turns and can be damped with a transverse feedback. The rise time was simulated to be quite larger than the calculated one (by a factor 5-10), as the simulation takes into account the real wiggler and the train length.

2.11.8 **Injection/Extraction**

The injection and extraction process is quite simple with only one pulse stored in the damping ring per cycle. This pulse contains two trains of 156 bunches with 1GHz structure. Each train which is supposed to be symmetrically spaced in the DR, covers a small fraction of the circumference of only 11%. The injection and extraction system is located at symmetric locations, at the end of the arc, after the dispersion suppressor and upstream of the super-conducting wigglers to avoid that synchrotron radiation damages the sensitive injection/extraction elements. The kickers can be placed at maximum horizontal beta functions for minimising the deflection angle. For the same reason, the phase advance between injection (extraction) septa and kickers are set to around $\pi/2$. Additional space can be added in order to install longer elements thus reducing the available voltage needed and accommodate protection systems.

An extraction kicker ripple produces a beam size jitter which is propagated up to the collider IP. On the other hand, injection kicker jitter is translated to reduction of the beam stay clear, during the injection process. For both processes, a typical tolerance of 10\% of the beam size at extraction or injection is considered, although in the case of injection, it can be relaxed to even higher values (e.g. 20-30%). Taking into account that the extracted beam size for the required normalised emittance of 500~nm corresponds to a few tens of microns, the kicker stability tolerance is around 10^{-4}.

A similar tolerance can be established for the kicker roll, which will induce a vertical beam size jitter. The extracted vertical beam size is of the order of a few μm and to keep the distortion to the order of a few hundred nm, the kicker alignment should be better than a few tens of μrad. Future refinement in the lattice of the damping rings will not change significantly the kicker specifications, especially the stringent required stability.

To ease this very tight requirement, a 2nd identical kicker powered by the same pulser can be installed in the extraction line, at a phase advance of π for jitter compensation. This solution was already proposed in the case of the NLC damping rings [1], which required similar stability tolerances. A double strip-line kicker system was at ATF with similar stability requirements but for shorter rise/fall times and flat top [27]. A prototype stripline kicker was built in collaboration with IFIC-Valencia and TRINOS and it is currently tested magentically at CERN [28]. There are plans on testing this stripline including the pulser in existing storage rings.

2.11.9 **Delay Loop**

The two trains of the CLIC DR have to be recombined in a single delay loop for both species, using RF deflectors. A unique α-shape loop, as in CTF3, is considered, for both species with a circumference of 263m, i.e. half of the damping rings. The optics is tuned to achieve high-order iso-chronism and is based on TME cells and sextupole tuning. The emittance growth due to synchrotron radiation is negligible due to the low energy and relatively short length of the loop. The path length correction is very critical and a wiggler, orbit correctors or a chicane may be considered in order to control it down to a few mm. The systematic energy loss is roughly half of the DR and can be corrected with RF cavities of a few hundred kV. As the beam stability requirement is quite low, this imposes tight jitter tolerances for the RF deflector (around 10^{-3} . This tolerance is within the capability of modern klystrons. It will necessitate a demonstration

through measurements in CTF3 which are equipped with similar RF deflectors for the drive beam recombination and frequency multiplication [29].

2.11.10 **Acknowledgements**

The author would like to thank all the members of the CLIC damping ring design team and the Low Emittance Rings collaborators for their numerous contributions to this work and in particular F. Antoniou, M. Barnes, S. Calatroni, P. Chiggiatto, R. Corsini, A. Grudiev, E. Koukovini-Platia, T. Lefevre, N. Mounet, G. Rumolo, S. Russenchuck, H. Schmickler, D. Schoerling, D. Schulte, M. Taborelli, G. Vandoni, M. Wendt, F. Zimmermann, P. Zisopoulos (CERN), Y.M. Boland, R. Dowd, R. Rassool, E. Tan, K. Wooton (ACAS, Melbourne, Australia), A. Bragin, E. Levichev, D. Shatilov, S. Siniatkin, S. Piminov, P. Vobbly, K. Zolotarev (BINP), M. Billing, J. Calvey, J. Crittenden, G. Dugan, D. Rubin, J. Shanks (Cornell), M. Palmer (FNAL), F. Torral (CIEMAT), M. Korostelev (Cockroft), C. Belver-Aguilar, A. Faus-Golfe (IFIC-Valencia), D. Alesini, M. Biagini, S. Guiducci, S. Liuzzo (INFN-LNF), P. Raimondi (ESRF), R. Bartolini (DIAMOND), K. Kubo, T. Naito, N. Terunuma, J. Urakawa (KEK-ATF), A. Bernard, A.S. Muller (KIT-ANKA), E. Wallen, A. Anderson (Maxlab), M. Aiba, M. Boege, N. Milas, L.Rivkin, A. Streun (PSI-SLS).

2.11.11 **References**

1. N. Phinney, N. Toge, N. Walker, ILC Reference Design Report Vol. 3 -Accelerator, arXiv:0712.2361, http://arxiv.org/pdf/0712.2361.pdf.
2. Next Linear Collider Zeroth-Order design report, SLAC-R-474, 2002.
3. 3rd Low Emittance Rings Workshop 2013, http://www.physics.ox.ac.uk/lowemittance13/index.asp
4. M. Aiba et al., Nuclear Instruments and Methods in Physics Research, 694, 2012.
5. F. Antoniou and Y. Papaphilippou, “Design considerations for the CLIC pre-damping rings”, PAC'09, Vancouver, May 2009.
6. H. Braun et al., CLIC 2008 parameters, CLIC-Note-764.
7. Y. Papaphilippou, H.H. Braun and M. Korostelev, “Parameter scan for the CLIC damping rings”, EPAC'08, Genova, June 2008, p.679.
8. F. Antoniou, M. Martini, Y. Papaphilippou and A. Vivoli, “Parameter scan for the CLIC Damping Rings under the influence of intrabeam scattering”, IPAC’10, Kyoto, 2010.
9. Y. Papaphilippou et al., “Lattice options for the CLIC damping rings”, PAC'09, Vancouver, May 2009.
10. Y. Papaphilippou et al., “Design Optimization for the CLIC Damping Rings”, IPAC2010, Kyoto, Japan, 2010.
11. Y. Renier et al. Proc. of IPAC 2011, p. 2205, San Sebastian, Spain, 2011.
12. K.P. Wooton, et al., Proc. of IPAC 2011, p. 1102, San Sebastian, Spain, 2011.
13. D. Schoerling et al, Design and System Integration of the Superconducting Wiggler Magnets for the CLIC Damping Rings, PRST-AB, 2012, (in press).
14. K. Zolotarev, et al., CLIC Note, 2009, in preparation.
15. A. Piwinski, Handbook of Accelerator Physics, World Scientific (1999) 125.
16. M. Martini, Tech. Rep. PS/84-9(A4), CERN, 1984.
17. J. Bjorken and S. Mtingwa, Part. Accel., 13 (1983) 115.
18. K. Bane, SLAC-PUB-9226, June 2002.
19. A. Vivoli and M. Martini, Proc. of IPAC 2010, p. , Kyoto, Japan, 2010.
20. M. Pivi et al, Proc. of IPAC 2012, p. 3147, New Orleans, USA, 2012.
21. M. Ehrichman et al, Proc. of IPAC 2012, p. 2970, New Orleans, USA, 2012.

22. F. Antoniou et al, Proc. of IPAC 2012, p. 1951, New Orleans, USA, 2012.
23. G. Rumolo, et al., "Electron Cloud Build Up and Instability in the CLIC Damping Rings", EPAC'08, Genova, June 2008.
24. E. Shaposhnikova, et al., "Experimental studies of carbon coatings as possible means of supressing beam induced electron multi-pacting in the CERN SPS", PAC'09, Vancouver, May 2009.
25. M. Palmer et al., "Electron Cloud at Low Emittance in CesrTA", IPAC'10, Kyoto, Japan, 2010.
26. N. Mounet and E. Metral, Proc. of IPAC 2011, p. 778, San Sebastian, Spain, 2011.
27. T. Naito et al, "Multi-bunch Beam Extraction by using Strip-line Kicker at KEK-ATF", IPAC'10, Kyoto, Japan, 2010.
28. C. Belver-Aguilar et al, IPAC 2013, 2013.
29. D. Alesini and F. Marcellini, "RF deflector design of the CLIC test facility CTF3 delay loop and beam loading effect analysis", PRSTAB12 031301, 2009.

2.12 High Frequency Studies for the CLIC Damping Rings

Eirini Koukovini-Platia, Giovanni Rumolo
CERN, CH 1211 Geneva 23, Switzerland; EPF Lausanne, Switzerland
Mail to: eirini.koukovini.platia@cern.ch

2.12.1 Introduction

Due to the unprecedented brilliance of the beams, the performance of the Compact Linear Collider (CLIC) damping rings (DR) is affected by collective effects. Single bunch instability thresholds and the associated coherent tune shifts have been evaluated with a multi-kick version of the HEADTAIL code in order to define the available transverse impedance budget. The study on the strip-line kickers and the electromagnetic material properties characterization at high frequencies will also be presented.

2.12.1.1 *HEADTAIL Simulations*

The interaction of charged particle beams with the surroundings, and therefore energy loss and transverse kick due to a particular machine element or the vacuum chamber, is expressed in terms of impedance in the frequency domain. The full ring is modeled with a total impedance made of two main components: resistive wall and one broad-band resonator. These interactions need to be known in order to estimate the thresholds of coherent instabilities which may limit the achievable beam current.

Single bunch instability thresholds and the associated coherent tune shifts have been evaluated with the HEADTAIL [1] code in the case where different impedance contributions are taken into account such as the broadband resonator in combination with the resistive wall contribution from the arc and the wigglers of the DR assuming the worst case scenario (in terms of impedance) of stainless steel (StSt) pipe coated with 2 μm of NEG. The DR parameters used for the simulations can be found in the CLIC DR twiki page [2].